

Form factor ratio from unpolarized elastic electron-proton scattering

Simone Pacetti

Dipartimento di Fisica e Geologia, and INFN Sezione di Perugia, 06123 Perugia, Italy

Egle Tomasi-Gustafsson*

IRFU, CEA, Université Paris-Saclay, 91191 Gif-sur-Yvette Cedex, France

(Received 8 April 2016; revised manuscript received 22 June 2016; published 29 November 2016)

A reanalysis of unpolarized electron-proton elastic scattering data is done in terms of the electric to magnetic form factor squared ratio. This observable is in principle more robust against experimental correlations and global normalizations. The present analysis shows indeed that it is a useful quantity that contains reliable and coherent information. The comparison with the ratio extracted from the measurement of the longitudinal to transverse polarization of the recoil proton in polarized electron-proton scattering shows that the results are compatible within the experimental errors. Limits are set on the kinematics where the physical information on the form factors can be safely extracted. The results presented in this work bring a decisive piece of information to the controversy on the deviation of the proton form factors from the dipole dependence.

DOI: [10.1103/PhysRevC.94.055202](https://doi.org/10.1103/PhysRevC.94.055202)

Hadron form factors (FFs) contain essential information on the electric and magnetic charge currents in the hadron and constitute a very convenient parametrization that enters in theoretical models and description of experimental observables concerning the three-leg vertex proton-proton-photon. It has been assumed for a long time that the proton electric FF, as well as the magnetic FFs of the proton and neutron, normalized to their magnetic moment, have a Q^2 -dipole dependence (Q is the four-momentum of the photon):

$$G_D(Q^2) = \left(1 + \frac{Q^2[\text{GeV}^2]}{0.71}\right)^{-2},$$

whereas the neutron electric FF is essentially zero. Evidence for the deviation of the proton electric FF from the dipole form was present since the 1970's, in experiments as well as in theory. However, the dipole parametrization was commonly accepted due to the following facts:

- (i) From the classical point of view, in the nonrelativistic approximation, FFs are Fourier transforms of the spatial densities of electric charge and magnetization of the nucleon; the dipole approximation corresponds to an exponential distribution, and the parameter 0.71 GeV^2 corresponds to a quite reasonable rms radius of the proton of 0.81 fm .
- (ii) FFs represent the probability that a proton remains in its ground state after receiving a momentum squared Q^2 , transferred by the virtual photon to one of its valence quarks and then transmitted to the others via gluon exchanges. From the QCD point of view, scaling laws predict a $(1/Q^2)^2$ dependence of the amplitude of the process [1,2] (corresponding to two gluon exchanges, the minimum number of exchanges needed for sharing the momentum among the three valence quarks).

The *reduced* cross section of electron-proton elastic scattering, in the Born approximation, i.e., by considering only one-photon exchange, σ_{red} , is linear in the variable $\epsilon = [1 + 2(1 + \tau)\tan^2(\theta_e/2)]^{-1}$, with θ_e the electron scattering angle in the proton rest frame and $\tau = Q^2/(4M^2)$, and it reads

$$\begin{aligned} \sigma_{\text{red}}(\theta_e, Q^2) &= \left[1 + 2\frac{E}{M}\sin^2(\theta_e/2)\right] \frac{4E^2\sin^4(\theta_e/2)}{\alpha^2\cos^2(\theta_e/2)} \\ &\quad \times \epsilon(1 + \tau)\frac{d\sigma}{d\Omega} \\ &= \epsilon G_E^2 + \tau G_M^2, \end{aligned} \quad (1)$$

where M is the proton mass, E and $d\sigma/d\Omega$ are the electron initial energy and the differential cross section in the proton rest frame, and G_E and G_M are the proton electric and magnetic Sachs FFs. The measurement of the differential (reduced) cross section at fixed Q^2 , for different angles, allows us to extract the squared values of the FFs, G_E^2 and G_M^2 , as the slope and the intercept (multiplied by τ), respectively, of this linear distribution (Rosenbluth separation [3]).

However, hints from experiments and theory cast some doubts on the accuracy of the dipole approximation:

In experiment. A series of measurements at moderate Q^2 at DESY [4] (single arm), at the Cambridge electron accelerator [5] with ep coincidence, and from proton and quasielastic deuteron scattering [6] found a decrease of the electric FF with Q^2 , with respect to the dipole, in the limit of the errors. In these experiments radiative corrections were either measured or controlled through a comparison between proton and deuteron targets, and never exceeded 20%. Further measurements at Mainz [7] as well as the Stanford Linear Accelerator Center (SLAC) experiment [8] showed also a deviation of the ratio $\mu G_E/G_M$ from unity, μ being the proton magnetic moment in units of the Bohr magneton. The aim to learn about nucleon structure up to the highest transferred momenta justified the extraction of G_M under the hypothesis $G_E = 0$ or $G_E = G_M/\mu$ [9], since in any case, the electric contribution to the unpolarized cross section is

*etomasi@cea.fr

suppressed by the factor τ with respect to the magnetic term. At larger Q^2 the large errors and other type of corrections, in particular radiative corrections, were applied following commonly accepted *Ansätze* and, in our opinion, not critically revised. Moreover, recent dedicated measurements at the Jefferson Lab [10], as well as reanalyses of existing data [11], confirmed the scaling FF behavior: $G_E \simeq G_M/\mu$.

In phenomenology. Typically the electric and magnetic distributions do not have to follow *a priori* similar Q^2 behavior. Moreover, magnetic and electric FFs of the neutron and proton may be different, since they do not have the same quark content. Some models predicted the decrease of the electric FF long before the data appeared, such as the two-component model of Ref. [12], built on vector meson dominance, or the soliton model [13] that attributed the decrease of the electric FF to approximations of relativistic effects, or the diquark model of Ref. [14].

The doubts on the deviation from the dipole became evident with the advent of polarization experiments. In the 1970's Akhiezer and Rekaló [15,16] showed that the polarization of the scattered proton in the scattering of longitudinally polarized electrons on an unpolarized target (or the asymmetry in the scattering of longitudinally polarized electrons on a transversely polarized target) contains an interference term proportional to the product $G_E G_M$. This observable would therefore be more sensitive to a small electric contribution, and even to its sign (particularly important for the neutron case). The suggested polarization method could be realized only recently, following the advent of high-intensity electron beams and large-acceptance detectors and thanks to tremendous progress in polarization techniques for beams, targets, and hadron polarimetry.

A measurement of the ratio of transverse and longitudinal polarization of the recoil proton gives a direct measurement of the ratio of electric and magnetic FFs, $R = G_E/G_M$:

$$\frac{P_t}{P_\ell} = -2 \cot(\theta_e/2) \frac{M_p}{E + E'} \frac{G_E}{G_M}, \quad (2)$$

and is free from systematic errors coming from the beam polarization and the analyzing powers of the polarimeter.

The data based on the Akhiezer-Rekaló method, mostly taken by the JLab GEp Collaboration ([17] and references therein), showed with unprecedented precision that the ratio of electric to magnetic FFs decreases as Q^2 increases. However, injecting the polarization ratio into the unpolarized cross section would modify G_M by 3% at most, within the experimental errors [18], showing that the problem is not at the level of the observables (i.e., unpolarized cross section and ratio of longitudinal to transverse proton polarization), within the experimental errors. Different conjectures or possible solutions to this problem have been discussed in the literature.

The experimental data were generally corrected by first-order radiative corrections, following the calculation for example, of Ref. [19]. This calculation contained approximations that were justified at small Q^2 and/or small acceptance detectors, but that may not hold at large incident and scattered electron energy and momentum, as well as at large momentum transfer. Radiative corrections become huge at large Q^2 especially for the unpolarized cross section. They are as large

for the polarized cross sections, but mostly cancel in the polarization ratio.

A revision removing some of these approximations was published [20], whereas a critical analysis of first-order calculations is available in Refs. [21,22]. New results on radiative corrections based on the lepton structure functions method, which takes into account higher orders in the leading logarithm approximation [23], can bring FF results in agreement [24]. This was confirmed later on by a more extended calculation, including hard photon emission [25]. Note that since the polarization data were made available, no experiment has been performed to verify the kinematics and the radiative emission with a precise measurement of the four-momenta of both outgoing particles and/or radiated particles in ep scattering. This would allow one to revise critically the assumptions and corrections applied to the previous (unpolarized) measurements.

The discrepancy was attributed by several authors to the presence of a two-photon exchange contribution. From that time, a lot of theoretical and experimental work has been devoted to this subject. Note that the two-photon contribution was already discussed in the literature in the 1970's [26–28] and recently discussed again: for ed elastic scattering [29] and ep elastic scattering [30]. A series of articles on model-independent properties of the two-photon contribution on different processes, i.e., ep scattering [31–33], $\bar{p}p \rightarrow e^+e^-$ [34], $e^+e^- \rightarrow \bar{p}p$ [35–37], e^-He^4 scattering, and $e^+e^- \rightarrow \pi^+\pi^-$ [38], showed clearly the consequences of the nonapplicability of the one-photon approximation, making necessary a serious revision of most of the obtained results. As an example, two-photon contributions would induce nonlinearities in the Rosenbluth fit as the hadronic current would be parametrized by three structure functions, of complex nature and depending on two kinematical variables, instead than by two real FFs functions of Q^2 . The extraction of the real FFs would still be possible, but requiring either polarized electron and positron beams, applying the Akhiezer-Rekaló method to the sum of the cross sections, where odd terms disappear; or measuring five T-even or three T-odd polarization observables, including triple spin observables, which appears very difficult.

Reanalysis of the e^+p/e^-p cross section ratio [39–41] gave negative results, as well as searches for non linearities of the reduced cross section, the slope of the Rosenbluth plot being driven by Q^2 and ϵ -dependent radiative corrections (the slope of the uncorrected cross section becoming even negative for $Q^2 > 2 \text{ GeV}^2$ [42]).

Model calculations of the two-photon exchange contribution were developed, giving quantitatively different results since the physical reasons for an enhancement of this term beyond the α -counting expectation differ essentially from one model to another [43–45]. Several measurements were proposed [46–48] and the results show that an asymmetry between electron and positron scattering exists indeed, and may reach 6–7%. However, most of the asymmetry comes from the interference between initial and final photon emission, and it is highly reduced when the data are properly radiatively corrected. The size of the additional two-photon contribution does not exceed the expected size from α counting (2–3%);

moreover, the measurements, being performed at low Q^2 , do not show evident increase with Q^2 . Note that an effect growing with Q^2 and reaching 6% at $Q^2 \simeq 6 \text{ GeV}^2$ is necessary to bring into agreement the data on the ratio G_E/G_M extracted from the Akhiezer-Rekalo and the Rosenbluth methods.

I. REANALYSIS OF EXISTING DATA

Problems of parameter correlations and limits inherent in the Rosenbluth method have been discussed in Ref. [49]. Previous global analyses were done, discussing in particular the problem of normalization among different sets of data and the omission of some of the data points [50], and reconsidering radiative corrections [21].

Here we suggest the following procedure to extract the FF information from the unpolarized cross sections. Instead of extracting separately G_E and G_M , we write the reduced cross section given in Eq. (1) as

$$\sigma_{\text{red}} = G_M^2 (R^2 \epsilon + \tau), \quad (3)$$

where G_M^2 and $R^2 = (G_E/G_M)^2$ are considered as independent parameters. The unpolarized data are fitted at fixed Q^2 . The procedure has the advantage of extracting directly the ratio, by automatically accounting for the effect of the correlations between G_E and G_M . The parameter R^2 represents directly the deviation of the linear dependence of the cross section from a constant in ϵ , whereas general normalization and systematic errors would be absorbed by G_M^2 . The results of the fit on the considered measurements of the unpolarized elastic ep cross section are summarized in Appendix A.

If, for some of the data, we recover values and errors consistent with the original publication, the data from Ref. [51] deserve a specific discussion. This work is especially representative, because it extends the individual FF extraction by the Rosenbluth method to the largest values of Q^2 .

The original cross-section data from [51] are reported in Appendix B, Table IV, and the individual fits at each Q^2 are illustrated in Fig. 6. The data of Ref. [51], with eight points and two settings, span the region $1.75 \leq Q^2 \leq 8.83 \text{ GeV}^2$. The two settings will be indicated as high-energy (HE) and low-energy (LE) experiments.

1. Analysis I

In the original paper the measured cross sections were published with the warning that an uncertainty of $\pm 5\%$ affected the second setting, due to a poor knowledge of the acceptance of the spectrometer. This error, however, was not added to the tabulated error. Instead, it was taken into account as a constant relative correction, according to the following procedure:

- (i) For the two lowest values $Q^2 = 1.75$ and 2.50 GeV^2 , the cross section was measured at each setting at the lowest ϵ , and showed a larger value from the LE setting by 4-5%.
- (ii) Assuming a linear ϵ dependence of the reduced cross section, i.e., the dominance of the one-photon exchange mechanism, a fit of the HE data was done

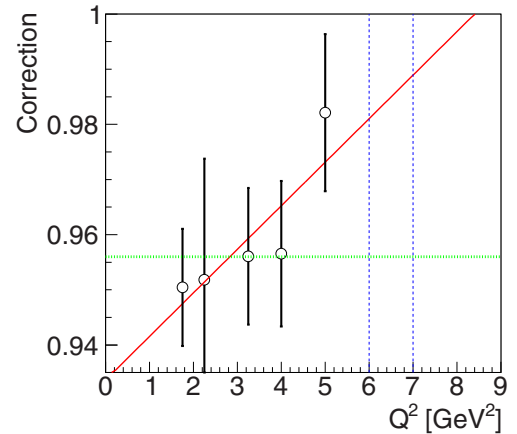


FIG. 1. Correction factor as a function of Q^2 . A linear fit (red line) shows an increasing of the factor. The dashed (blue) lines indicate that the extrapolated correction for the two HE points would be close to 1% rather than $\simeq 5\%$, as applied in the original paper.

and the LE energy point was renormalized to lie on the straight line.

- (iii) The same constant normalization $C = 0.956$, fixed on the low Q^2 point, was applied to the cross section at all Q^2 .

This procedure has the effect of enhancing the slope, thus increasing the FF ratio. Note that for $Q^2 = 6$ and 7 GeV^2 only two points are present. The renormalization (lowering) of the first point changes essentially the slope of the linear fit.

2. Analysis II

We recalculate the ratio using the data as published, without renormalizing the two settings and considering the LE points as additional independent measurements. In this case the data points at $Q^2 = 1.75$ and 2.5 GeV^2 are both included in the fit, constraining the fit to an average value.

3. Analysis III

We fit only the HE points (excluding therefore the two measurements at $Q^2 = 6$ and 7 GeV^2). We find a slope consistent with analysis II, although affected by larger errors, as the number of points is smaller.

4. Analysis IV

We repeat the normalization procedure, by aligning the LE point on the straight line fitting the HE points. We note a systematic increase of the normalization factor (Fig. 1, and Table I). It is well known that the acceptance of a spectrometer depends on the kinematics of the particle, and it is not surprising that the needed corrections decrease at large energies ($C \rightarrow 1$). Applying a normalization coefficient that is not constant with Q^2 but derived in order to align the LE point to the straight line defined by the HE points turns out to be equivalent to analysis III in terms of slope and intercept. This explains the agreement between analyses III and IV.

The results are reported in Fig. 2 and compared to the ratio from polarization data. We may conclude that the results from

TABLE I. Normalization factor for the LE point derived from a linear fit of the HE points. The data are those of Ref. [51]. The numbers with the superscript * are directly derived from the ratio of the measured cross sections.

Q^2 (GeV ²)	Correction
1.75*	0.951144 ± 0.0156952
1.75	0.950432 ± 0.0106094
2.25*	0.955992 ± 0.0259077
2.25	0.951849 ± 0.0219368
3.25	0.956075 ± 0.0123809
4	0.956552 ± 0.0131748
5	0.982138 ± 0.0142443

analyses II, III, and IV are consistent with the decreasing of the ratio indicated by the polarization data. Therefore a revision of the normalization factor brings the data into agreement. Moreover, in light of all the above, it is nonsense to use the FF data from Ref. [51] to probe the two-photon effect, because they were extracted under the hypothesis of linearity of the reduced cross section, i.e., correcting the first point to be aligned. The results showed consistency with the hypothesis $\mu^2 R^2 \simeq 1$ at large Q^2 , as expected at that time. The tendency of the first two points to deviate from unity was operatively corrected by the renormalization procedure.

II. ANALYSIS AND DISCUSSION OF AVAILABLE DATA

A complete discussion and data basis of unpolarized and polarized measurements can be found in Ref. [52]. There, it was already noted that some unpolarized data, where radiative corrections were lower than 20%, indeed showed a deviation of the ratio $\mu^2 R^2$ from unity consistent with the polarization data.

We consider below only the cross-section data where the individual determination of FFs was done and the ratio was

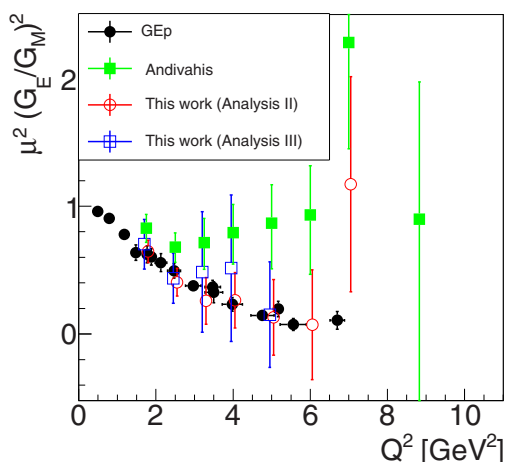


FIG. 2. $\mu^2 R^2 = \mu^2(G_E/G_M)^2$ as a function of Q^2 from Andivahis [51] as originally published, from analysis II without renormalization, and from analysis III omitting the lowest ϵ point, compared with the values from polarization experiments (GEp [17]).

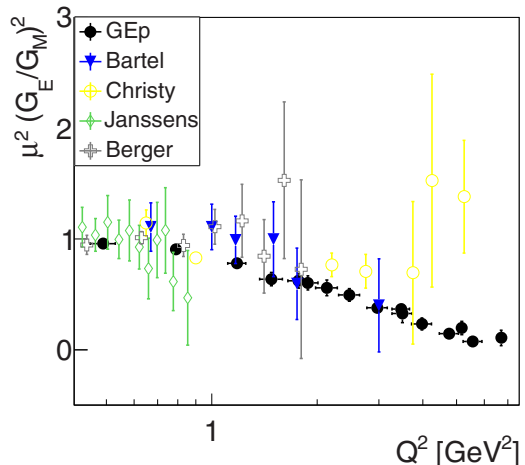


FIG. 3. $\mu^2 R^2 = \mu^2(G_E/G_M)^2$ as a function of Q^2 from Bartel [4], Christy [11], Janssens [53], and Berger [54] compared with the values from polarization experiments (GEp [17]).

extracted from a Rosenbluth separation. The main set of data considered in this analysis is the one collected in Ref. [52], with a focus on the region $Q^2 \geq 1$ GeV², which includes 64 data points.

Data obtained from unpolarized ep elastic scattering as reported in Refs. [4,11,53,54], showing a squared ratio consistent with the polarization data, in the limit of the (large) errors, are illustrated in Fig. 3. The corresponding data are reported in Appendixes C–F, the cross sections are given in Tables V–VIII, and the individual fits at each Q^2 are illustrated in Figs. 7–10.

The other parameter of the fit, G_M^2 , normalized to the dipole and to the proton magnetic moments (squared), is shown in Fig. 4. These results are important for consistency check, in order to corroborate the suggested procedure.

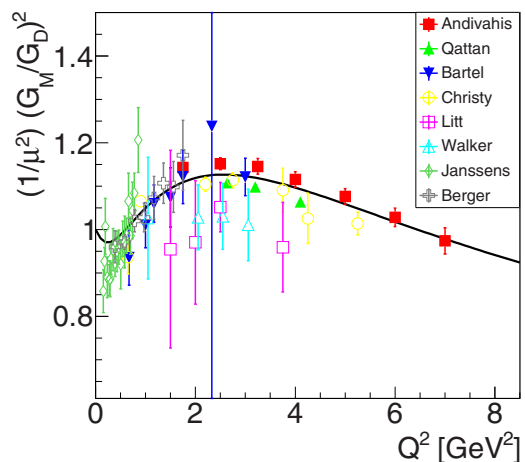


FIG. 4. Magnetic FF (normalized to μ and to the dipole) squared as a function of Q^2 . Data are from Andivahis [51], Bartel [4], Christy [11], Janssens [53], Berger [54], Qattan [10], Walker [56], and Litt [9], compared with the calculation of Ref. [55], chosen as an example (black solid line).

They are compared to the vector meson dominance model of Ref. [55] (black solid line), chosen as an example. As expected, the magnetic FF is better determined by the Rosenbluth fit, and the present values are consistent with the model that represents, in fact, a global fit to the data. The numerical values are reported in Appendix A and Table II. Among the available data, three sets [9,10,56] show a particular behavior that is not consistent with the previous finding, giving a value of the ratio exceeding unity and growing with Q^2 . The numbers are reported in Appendixes G–I, the cross sections in Tables IX–XI, and the individual fits at each Q^2 are illustrated in Figs. 11–13.

For these experiments it was noted in Ref. [49] that radiative corrections and/or correlations are especially large. The data from Ref. [10] were extracted detecting the proton instead of the electron. Besides the above-mentioned corrections, at large Q^2 the contamination of the elastic peak by the inelastic $e + p \rightarrow e + p + \pi^0$ reaction had to be carefully subtracted [17].

For Refs. [9,56], G_M^2 extracted from the present analysis is systematically lower, showing that these measurements may be affected by a global systematic error probably due to normalization issues, whereas the results of Ref. [10] agree with the standard parametrization of the magnetic contribution.

Note that in Ref. [9] a somehow arbitrary renormalization was done by “changing the normalization of the small angle data from SLAC or DESY by $\pm 1.5\%$ with respect to the large angle data (Bonn)”. This normalization increased the FF ratio toward unity.

The complete set of results in the form of tables is given in the appendixes. Concerning, in general, the elastic ep cross section, several early experiments pointed out a deviation of the elastic cross section from the $(1/Q^2)^5$ behavior. Quoting a presentation of the data at the highest available transferred momenta, from Nobel prize winner R. Taylor: “There appears to be definite evidence in the data for a significant deviation from the dipole fit” [57]. Radiative corrections were also quoted as a point to be treated with particular attention.

The dipole normalized cross section

$$\frac{\sigma}{\sigma_D} = \frac{\sigma_{\text{red}}^{\text{expt}}}{G_D^2(\epsilon/\mu^2 + \tau)},$$

with $\sigma_{\text{red}}^{\text{expt}}$ the measured reduced cross section, is reported in Fig. 5 as a function of Q^2 , regardless of the value of ϵ . The Q^2 coordinates for the data from a Rosenbluth separation for different ϵ are seen as vertically quasialigned symbols. Note that if these points form a cluster with overlapping error bars, it means that they are compatible with the relation $G_E \simeq G_M/\mu \simeq G_D$. If points are not overlapping, then FFs do not follow a dipole behavior. Concerning the data of Ref. [51], let us note that the dispersion at fixed Q^2 is not larger than the systematics from different sets.

In general, and particularly at large Q^2 , one can see that the dipole fit is not a good representation of the data. The deviation at large Q^2 reaches 20–30% on the cross section and has to be attributed mainly to the magnetic term. This is very

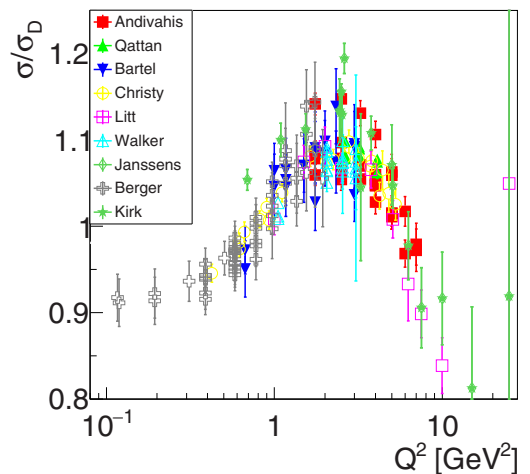


FIG. 5. Cross section normalized to the dipole cross section, σ/σ_D , as a function of Q^2 for different experiments: Andivahis [51], Qattan [10], Bartel [4], Christy [11], Litt [9], Walker [56], Janssens [53], Berger [54], Kirk [58].

puzzling, since it is expected that the magnetic FF follows quark counting rules that are compatible with the Q^2 dipole dependence.

III. CONCLUSIONS

We have proposed a reanalysis of the Rosenbluth data in terms of the squared FF ratio R^2 instead that of the extraction of the individual FFs, similar to what has been done in the time-like region. In such a region, this procedure is more convenient because of the scarce statistics; in the present case it allows us to consider R^2 as a parameter, directly extracted, avoiding the correlations between G_E^2 , which is affected by large error bars, and G_M^2 , which here includes the eventual systematics and global normalization problems. We have interpreted our results as follows. In general, the discrepancy between unpolarized and polarized experiments is not evident for the older experiments. Most of them show a decrease of the ratio, already noted in the literature. Up to 3–4 GeV^2 the eventual difference may be resolved by a proper calculation of radiative corrections.

Claiming the presence of two-photon contributions, correcting the unpolarized cross section by the assumed effect and extracting the FFs as real quantities, functions of one variable Q^2 , is in principle erroneous, because it integrates the conceptual and operative contradiction of merging the Born approximation and the two-photon effects. In the presence of two-photon effects one cannot extract nucleon FFs from the unpolarized cross section only.

In conclusion, in all these analyses the FF extraction is based on the dominance of the one-photon exchange mechanism. Advocating a large contribution of the $1\gamma - 2\gamma$ interference would invalidate the definition of FF itself as a real function of the single variable Q^2 . For a specific set of data [51], we have shown that considering two spectrometer settings as independent measurements brings these data into agreement with the data from the JLab GEp Collaboration. Omitting the

TABLE II. Comparison between our results and published values from Refs. [4,51,53].

Data set	q^2 (GeV ²)	This work		Original	
		$\mu^2(R^2 \pm \delta R^2)$	$\frac{G_M^2 \pm \delta G_M^2}{\mu^2 G_D^2}$	$\mu^2(R^2 \pm \delta R^2)$	$\frac{G_M^2 \pm \delta G_M^2}{\mu^2 G_D^2}$
Ref. [51]	1.75	0.648 ± 0.089	1.140 ± 0.014	0.828 ± 0.109	1.102 ± 0.021
	2.50	0.414 ± 0.108	1.148 ± 0.014	0.679 ± 0.115	1.111 ± 0.015
	3.25	0.260 ± 0.183	1.142 ± 0.018	0.716 ± 0.200	1.092 ± 0.019
	4.00	0.264 ± 0.211	1.111 ± 0.018	0.794 ± 0.233	1.063 ± 0.019
	5.00	0.131 ± 0.295	1.074 ± 0.018	0.867 ± 0.330	1.024 ± 0.018
	6.00	0.073 ± 0.429	1.028 ± 0.021	0.931 ± 0.426	0.974 ± 0.024
	7.00	1.171 ± 0.841	0.971 ± 0.030	2.280 ± 0.788	0.920 ± 0.031
Ref. [53]	0.16	1.224 ± 0.126	0.858 ± 0.050	1.223 ± 0.098	0.858 ± 0.050
	0.18	0.975 ± 0.076	0.925 ± 0.031	1.013 ± 0.060	0.918 ± 0.030
	0.19	0.937 ± 0.129	1.007 ± 0.065	0.939 ± 0.104	1.007 ± 0.068
	0.23	1.176 ± 0.133	0.886 ± 0.048	1.172 ± 0.099	0.886 ± 0.047
	0.27	1.130 ± 0.125	0.881 ± 0.035	1.131 ± 0.102	0.881 ± 0.036
	0.29	1.141 ± 0.145	0.884 ± 0.040	1.140 ± 0.113	0.884 ± 0.041
	0.31	0.944 ± 0.111	0.930 ± 0.036	0.945 ± 0.091	0.930 ± 0.036
	0.35	0.933 ± 0.162	0.950 ± 0.049	0.933 ± 0.128	0.950 ± 0.048
	0.39	1.129 ± 0.123	0.918 ± 0.031	1.124 ± 0.098	0.920 ± 0.032
	0.43	1.103 ± 0.181	0.947 ± 0.047	1.103 ± 0.148	0.949 ± 0.045
	0.47	1.041 ± 0.149	0.955 ± 0.039	1.046 ± 0.122	0.953 ± 0.038
	0.51	1.148 ± 0.242	0.918 ± 0.057	1.139 ± 0.281	0.921 ± 0.084
	0.55	0.989 ± 0.174	0.978 ± 0.041	0.994 ± 0.184	0.975 ± 0.049
	0.58	1.057 ± 0.274	0.975 ± 0.060	1.048 ± 0.380	0.973 ± 0.098
	0.62	0.918 ± 0.197	0.987 ± 0.041	0.924 ± 0.168	0.988 ± 0.042
	0.66	0.712 ± 0.287	1.067 ± 0.065	0.714 ± 0.253	1.070 ± 0.062
	0.70	1.199 ± 0.265	0.976 ± 0.041	1.201 ± 0.233	0.975 ± 0.039
0.74	1.077 ± 0.386	1.044 ± 0.065	1.075 ± 0.337	1.044 ± 0.068	
0.78	0.627 ± 0.265	1.082 ± 0.046	0.623 ± 0.489	1.086 ± 0.092	
0.86	0.555 ± 0.345	1.186 ± 0.050	0.549 ± 0.497	1.189 ± 0.074	
Ref. [4]	0.67	1.109 ± 0.162	0.923 ± 0.049	1.110 ± 0.160	0.933 ± 0.060
	1.00	1.108 ± 0.205	1.015 ± 0.052	1.090 ± 0.210	1.036 ± 0.059
	1.17	0.989 ± 0.153	1.041 ± 0.032	0.990 ± 0.150	1.057 ± 0.043
	1.50	0.999 ± 0.270	1.048 ± 0.056	1.000 ± 0.270	1.069 ± 0.064
	1.75	0.608 ± 0.207	1.088 ± 0.033	0.600 ± 0.210	1.118 ± 0.044
	2.00	− 4.405 ± 0.010	1.525 ± 0.044	0.650 ± 0.210	1.110 ± 0.042
	2.33	− 1.409 ± 0.199	1.200 ± 0.045	0.510 ± 0.280	1.131 ± 0.047
3.00	0.409 ± 0.418	1.069 ± 0.050	0.400 ± 0.320	1.115 ± 0.046	

low-energy data also brings the data into agreement, but at the price of increasing the error. The question arises then regarding the normalization procedure adopted in that paper. The *Ansatz* of constant normalization fixed on one low- ϵ point on the value that aligns the points at a fixed Q^2 is very critical to increasing

the Rosenbluth slope. The question remains open in light of the recent and precise JLab data from Ref. [10], which show three aligned values for the ratio increasing with Q^2 , as well as the data of Refs. [9,56], showing a similar increase although with large errors.

APPENDIX A: RESULTS FOR R^2 AND G_M^2

The obtained values for the parameters R^2 and G_M^2 in comparison with the corresponding values published in the original analyses [4,9–11,51,53,54,56] are reported in Tables II and III.

APPENDIX B: FIT OF THE DATA OF REF. [51]

Table IV reports the original data from Ref. [51]. Fits to these data, for the eight Q^2 values, are shown in Fig. 6.

APPENDIX C: FIT OF THE DATA OF REF. [53]

Table V reports the original data from Ref. [53]. Fits to these data for 20 Q^2 values are shown in Fig. 7.

TABLE III. Comparison between our results and published values from Refs. [4,9–11,54,56].

Data set	q^2 (GeV ²)	This work		Original	
		$\mu^2(R^2 \pm \delta R^2)$	$\frac{G_M^2 \pm \delta G_M^2}{\mu^2 G_D^2}$	$\mu^2(R^2 \pm \delta R^2)$	$\frac{G_M^2 \pm \delta G_M^2}{\mu^2 G_D^2}$
Ref. [54]	0.12	2.603 ± 13.244	0.406 ± 1.855		
	0.19	1.371 ± 3.302	0.734 ± 1.296		
	0.39	0.915 ± 0.083	0.973 ± 0.037	0.943 ± 0.089	0.960 ± 0.039
	0.58	0.977 ± 0.054	0.973 ± 0.017	0.976 ± 0.053	0.973 ± 0.017
	0.78	0.902 ± 0.097	1.014 ± 0.025	0.910 ± 0.076	1.013 ± 0.022
	0.97	1.065 ± 0.152	1.015 ± 0.033	0.949 ± 0.103	1.033 ± 0.027
	1.17	1.099 ± 0.318	1.057 ± 0.048	0.762 ± 0.122	1.102 ± 0.032
	1.36	0.787 ± 0.320	1.085 ± 0.046	0.832 ± 0.146	1.081 ± 0.034
	1.56	1.444 ± 0.683	1.073 ± 0.057	0.686 ± 0.151	1.130 ± 0.035
	1.75	0.661 ± 0.776	1.142 ± 0.078	0.590 ± 0.194	1.148 ± 0.044
	Ref. [56]	1.00	0.991 ± 0.486	1.023 ± 0.136	0.969 ± 0.172
2.00		1.311 ± 0.467	1.024 ± 0.073	1.338 ± 0.224	1.028 ± 0.044
2.50		1.336 ± 0.583	1.030 ± 0.074	1.143 ± 0.265	1.061 ± 0.044
3.01		1.563 ± 0.777	1.008 ± 0.080	1.480 ± 0.409	1.024 ± 0.050
Ref. [9]	1.00	− 0.587 ± 0.693	1.926 ± 0.750	0.941 ± 0.097	
	1.50	1.581 ± 1.218	0.953 ± 0.221	0.672 ± 0.131	
	2.00	1.665 ± 0.997	0.969 ± 0.142	1.124 ± 0.360	
	2.50	1.170 ± 0.419	1.039 ± 0.057	1.346 ± 0.441	
	3.75	2.308 ± 0.862	0.957 ± 0.073	1.988 ± 0.874	
Ref. [11]	0.65	1.144 ± 0.118	0.937 ± 0.039	1.143 ± 0.182	1.071 ± 0.108
	0.90	0.830 ± 0.011	1.065 ± 0.004	0.861 ± 0.124	0.910 ± 0.101
	2.20	0.766 ± 0.107	1.104 ± 0.016	0.771 ± 0.220	0.852 ± 0.223
	2.75	0.709 ± 0.153	1.113 ± 0.017	0.707 ± 0.183	0.789 ± 0.202
	3.75	0.695 ± 0.643	1.090 ± 0.051	0.701 ± 0.368	0.762 ± 0.405
	4.25	1.526 ± 0.961	1.026 ± 0.058	1.538 ± 0.404	1.575 ± 0.394
	5.25	1.382 ± 0.508	1.014 ± 0.026	1.383 ± 1.298	1.399 ± 1.209
Ref. [10]	2.64	0.817 ± 0.058	1.104 ± 0.006	0.814 ± 0.069	1.109 ± 0.032
	3.20	0.947 ± 0.087	1.093 ± 0.007	0.924 ± 0.098	1.098 ± 0.031
	4.10	1.266 ± 0.161	1.058 ± 0.009	1.203 ± 0.169	1.063 ± 0.031

TABLE IV. Reduced cross sections from Ref. [51].

Q^2 (GeV ²)	ϵ	σ_{red}	Q^2 (GeV ²)	ϵ	σ_{red}
1.75	0.250	0.032703 ± 0.000365	4.00	0.190	0.005172 ± 0.000071
1.75	0.250	0.031105 ± 0.000378	4.00	0.437	0.005063 ± 0.000088
1.75	0.704	0.034287 ± 0.000363	4.00	0.593	0.005117 ± 0.000081
1.75	0.950	0.035499 ± 0.000411	4.00	0.694	0.005231 ± 0.000083
2.50	0.227	0.015839 ± 0.000181	4.00	0.805	0.005133 ± 0.000069
2.50	0.227	0.015142 ± 0.000216	4.00	0.946	0.005303 ± 0.000069
2.50	0.479	0.015540 ± 0.000208	5.00	0.171	0.002859 ± 0.000041
2.50	0.630	0.015766 ± 0.000209	5.00	0.389	0.002904 ± 0.000066
2.50	0.750	0.016112 ± 0.000174	5.00	0.538	0.002819 ± 0.000050
2.50	0.820	0.016239 ± 0.000187	5.00	0.704	0.002849 ± 0.000041
2.50	0.913	0.016282 ± 0.000194	5.00	0.919	0.002902 ± 0.000043
3.25	0.206	0.008660 ± 0.000112	6.00	0.156	0.001715 ± 0.000029
3.25	0.426	0.008438 ± 0.000132	6.00	0.886	0.001721 ± 0.000028
3.25	0.609	0.008646 ± 0.000113	7.00	0.847	0.001152 ± 0.000029
3.25	0.719	0.008759 ± 0.000114	7.00	0.143	0.001094 ± 0.000028
3.25	0.865	0.008793 ± 0.000098	8.83	0.125	0.000530 ± 0.000022

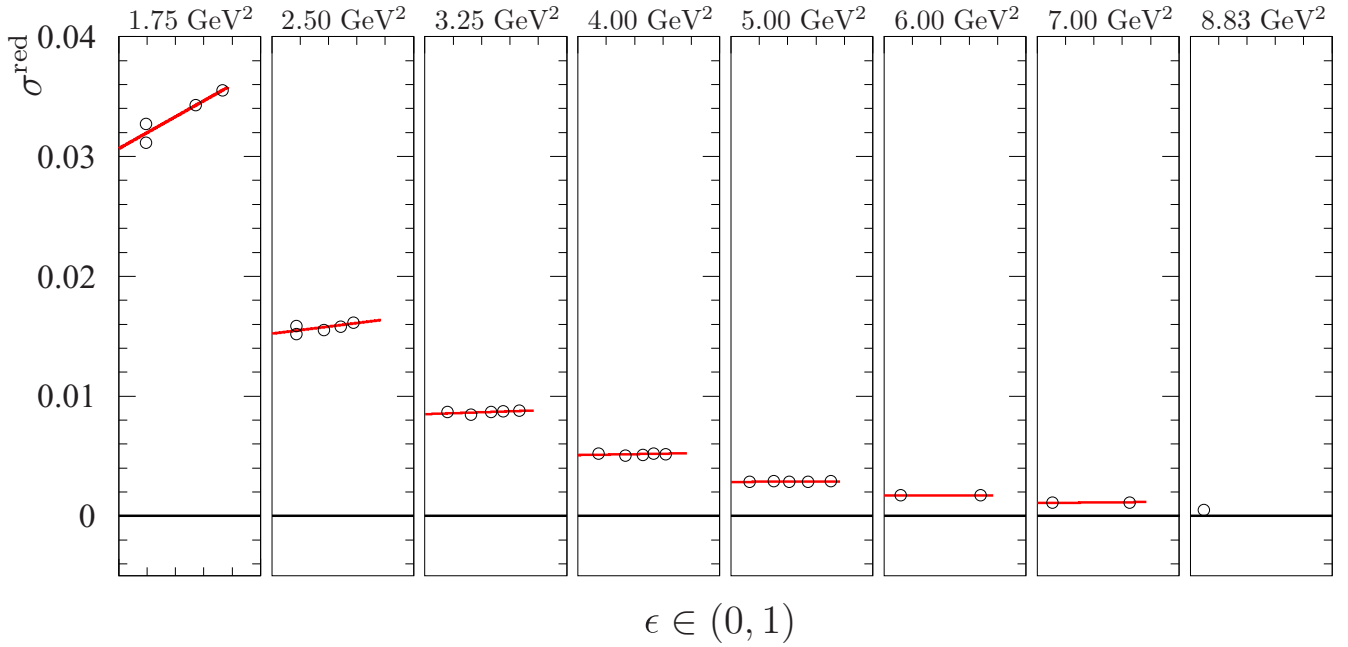


FIG. 6. Graphs representing data (open circles) from Ref. [51] and fits (red lines) of the reduced cross section as a function of ϵ , at the Q^2 values reported at the top of each graph.

TABLE V. Reduced cross sections from Ref. [53].

Q^2 (GeV ²)	ϵ	σ_{red}	Q^2 (GeV ²)	ϵ	σ_{red}	Q^2 (GeV ²)	ϵ	σ_{red}
0.16	0.736	0.4882 ± 0.0192	0.31	0.044	0.1640 ± 0.0082	0.62	0.541	0.1514 ± 0.0076
0.16	0.449	0.3433 ± 0.0136	0.35	0.577	0.2487 ± 0.0127	0.62	0.492	0.1477 ± 0.0075
0.16	0.076	0.1704 ± 0.0067	0.35	0.436	0.2276 ± 0.0091	0.62	0.419	0.1332 ± 0.0064
0.18	0.735	0.4356 ± 0.0178	0.35	0.072	0.1609 ± 0.0065	0.62	0.376	0.1408 ± 0.0071
0.18	0.588	0.3448 ± 0.0148	0.39	0.709	0.2747 ± 0.0134	0.62	0.068	0.1139 ± 0.0057
0.18	0.447	0.3180 ± 0.0127	0.39	0.575	0.2387 ± 0.0096	0.62	0.041	0.1135 ± 0.0057
0.18	0.322	0.2676 ± 0.0132	0.39	0.433	0.2117 ± 0.0087	0.66	0.506	0.1430 ± 0.0072
0.18	0.137	0.1959 ± 0.0098	0.39	0.310	0.1955 ± 0.0097	0.66	0.417	0.1317 ± 0.0064
0.18	0.075	0.1808 ± 0.0072	0.39	0.131	0.1594 ± 0.0080	0.66	0.067	0.1164 ± 0.0058
0.18	0.045	0.1642 ± 0.0066	0.39	0.072	0.1505 ± 0.0060	0.68	0.416	0.1325 ± 0.0055
0.19	0.776	0.4308 ± 0.0213	0.39	0.043	0.1480 ± 0.0074	0.70	0.470	0.1375 ± 0.0068
0.19	0.446	0.3388 ± 0.0169	0.43	0.707	0.2536 ± 0.0127	0.70	0.415	0.1288 ± 0.0065
0.19	0.075	0.1896 ± 0.0094	0.43	0.431	0.1981 ± 0.0097	0.70	0.372	0.1200 ± 0.0058
0.23	0.727	0.4055 ± 0.0202	0.43	0.071	0.1482 ± 0.0059	0.70	0.067	0.1021 ± 0.0051
0.23	0.585	0.3366 ± 0.0137	0.47	0.675	0.2248 ± 0.0115	0.70	0.040	0.1012 ± 0.0051
0.23	0.443	0.2888 ± 0.0146	0.47	0.639	0.2158 ± 0.0109	0.74	0.434	0.1229 ± 0.0063
0.23	0.074	0.1727 ± 0.0069	0.47	0.428	0.1830 ± 0.0073	0.74	0.412	0.1312 ± 0.0080
0.27	0.582	0.3072 ± 0.0125	0.47	0.070	0.1396 ± 0.0069	0.74	0.066	0.1025 ± 0.0051
0.27	0.441	0.2707 ± 0.0109	0.47	0.042	0.1381 ± 0.0069	0.78	0.410	0.1197 ± 0.0060
0.27	0.280	0.2060 ± 0.0103	0.49	0.427	0.1722 ± 0.0068	0.78	0.397	0.1213 ± 0.0058
0.27	0.074	0.1637 ± 0.0065	0.51	0.642	0.2079 ± 0.0103	0.78	0.368	0.1015 ± 0.0049
0.27	0.044	0.1635 ± 0.0082	0.51	0.426	0.1647 ± 0.0068	0.78	0.337	0.0996 ± 0.0049
0.29	0.581	0.2924 ± 0.0120	0.51	0.070	0.1305 ± 0.0065	0.78	0.066	0.1098 ± 0.0054
0.29	0.440	0.2570 ± 0.0105	0.55	0.609	0.1955 ± 0.0098	0.78	0.039	0.0927 ± 0.0046
0.29	0.316	0.2234 ± 0.0113	0.55	0.567	0.1774 ± 0.0092	0.86	0.406	0.1130 ± 0.0056
0.29	0.133	0.1733 ± 0.0087	0.55	0.424	0.1542 ± 0.0064	0.86	0.324	0.0945 ± 0.0056
0.29	0.073	0.1653 ± 0.0066	0.55	0.069	0.1258 ± 0.0063	0.86	0.065	0.0995 ± 0.0050
0.31	0.626	0.2746 ± 0.0136	0.55	0.041	0.1301 ± 0.0065	0.86	0.038	0.0951 ± 0.0047
0.31	0.580	0.2674 ± 0.0132	0.58	0.575	0.1770 ± 0.0087	1.01	0.037	0.0725 ± 0.0039
0.31	0.438	0.2433 ± 0.0095	0.58	0.421	0.1444 ± 0.0074	1.09	0.037	0.0630 ± 0.0044
0.31	0.073	0.1606 ± 0.0064	0.58	0.069	0.1227 ± 0.0062	1.17	0.036	0.0551 ± 0.0044

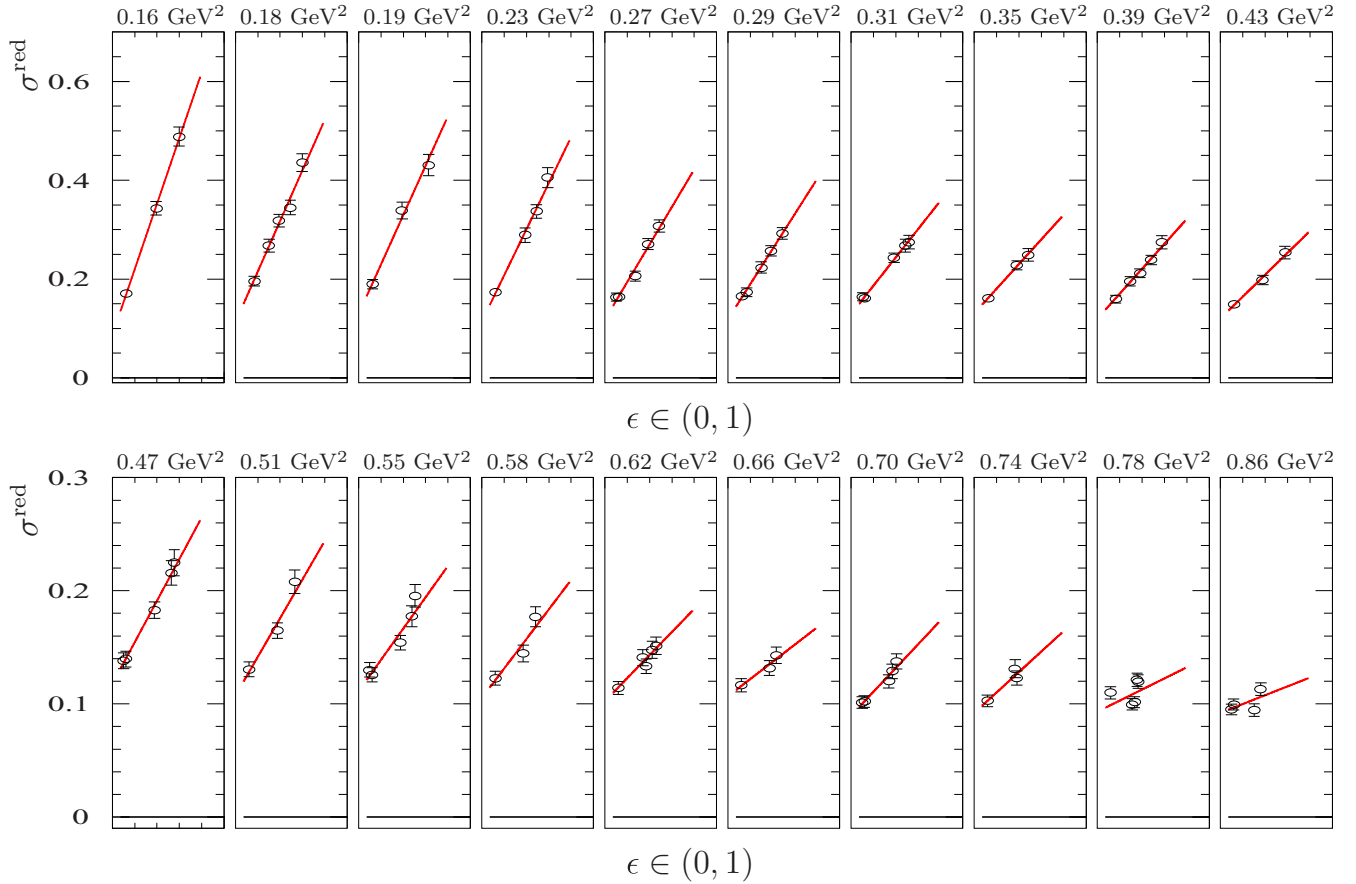


FIG. 7. Same as Fig. 6, but for data from Ref. [53].

APPENDIX D: FIT OF THE DATA OF REF. [4]

Table VI reports the original data from Ref. [4]. Fits to these data for the eight Q^2 values are shown in Fig. 8.

TABLE VI. Reduced cross sections from Ref. [4].

Q^2 (GeV ²)	ϵ	σ_{red}	Q^2 (GeV ²)	ϵ	σ_{red}
0.67	0.974	0.16589 ± 0.00315	1.75	0.965	0.03371 ± 0.00081
0.67	0.326	0.11937 ± 0.00322	1.75	0.250	0.03048 ± 0.00098
1.00	0.972	0.09933 ± 0.00209	1.75	0.278	0.03052 ± 0.00076
1.00	0.309	0.07717 ± 0.00224	2.00	0.948	0.00181 ± 0.00004
1.17	0.969	0.07534 ± 0.00143	2.00	0.268	0.02334 ± 0.00065
1.17	0.273	0.06127 ± 0.00165	2.33	0.952	0.01364 ± 0.00035
1.17	0.301	0.06081 ± 0.00152	2.33	0.257	0.01714 ± 0.00050
1.50	0.970	0.04791 ± 0.00096	3.00	0.918	0.01006 ± 0.00021
1.50	0.287	0.04030 ± 0.00137	3.00	0.237	0.00966 ± 0.00033

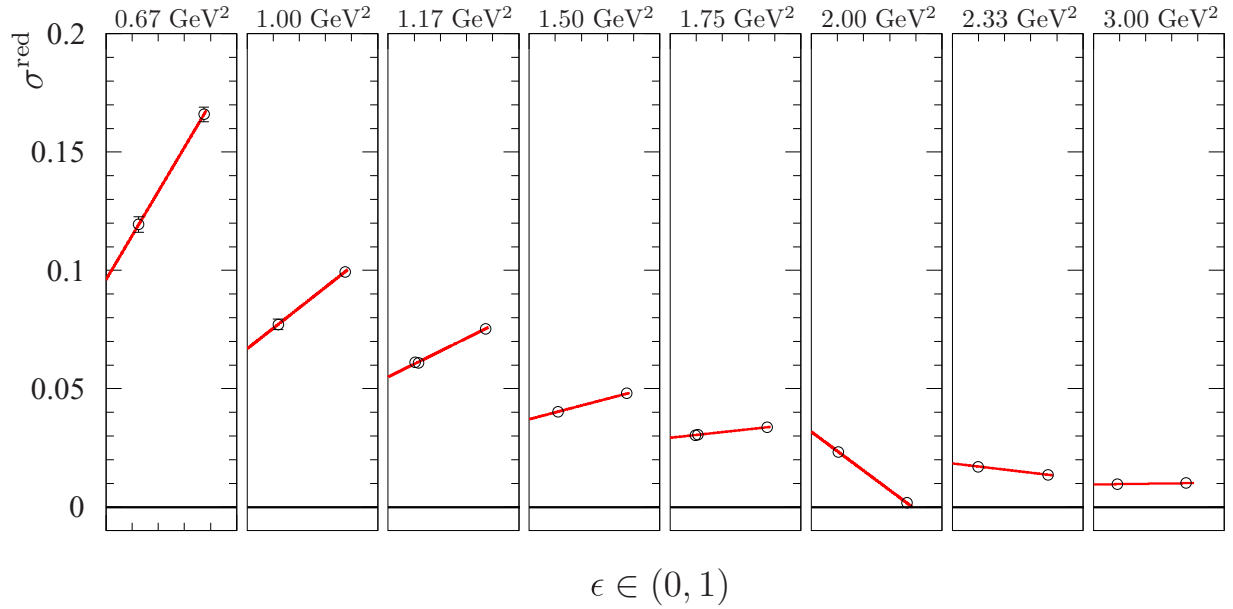


FIG. 8. Same as Fig. 6, but for data from Ref. [4].

APPENDIX E: FIT OF THE DATA OF REF. [54]

Table VII reports the original data from Ref. [54]. Fits to these data, for eight Q^2 values, are shown in Fig. 9.

APPENDIX F: FIT OF THE DATA OF REF. [11]

Table VIII reports the original data from Ref. [11]. Fits to these data for the seven Q^2 values are shown in Fig. 10.

TABLE VII. Reduced cross sections from Ref. [54].

Q^2 (GeV ²)	ϵ	σ_{red}	Q^2 (GeV ²)	ϵ	σ_{red}	Q^2 (GeV ²)	ϵ	σ_{red}
0.08	0.907	0.6535 ± 0.0197	0.58	0.810	0.1858 ± 0.0037	0.97	0.499	0.0862 ± 0.0020
0.12	0.906	0.5782 ± 0.0171	0.58	0.720	0.1740 ± 0.0035	0.97	0.281	0.0801 ± 0.0020
0.12	0.828	0.5334 ± 0.0161	0.58	0.663	0.1684 ± 0.0034	0.97	0.161	0.0732 ± 0.0025
0.19	0.904	0.4656 ± 0.0144	0.58	0.644	0.1713 ± 0.0035	1.17	0.736	0.0729 ± 0.0029
0.19	0.825	0.4354 ± 0.0131	0.58	0.522	0.1596 ± 0.0032	1.17	0.489	0.0679 ± 0.0015
0.31	0.901	0.3471 ± 0.0086	0.58	0.516	0.1573 ± 0.0032	1.17	0.272	0.0616 ± 0.0016
0.39	0.900	0.2884 ± 0.0058	0.58	0.300	0.1401 ± 0.0031	1.17	0.155	0.0611 ± 0.0031
0.39	0.848	0.2727 ± 0.0053	0.58	0.298	0.1402 ± 0.0028	1.36	0.623	0.0518 ± 0.0014
0.39	0.843	0.2788 ± 0.0055	0.58	0.173	0.1274 ± 0.0029	1.36	0.473	0.0522 ± 0.0019
0.39	0.818	0.2758 ± 0.0056	0.58	0.170	0.1302 ± 0.0027	1.36	0.263	0.0485 ± 0.0016
0.39	0.674	0.2468 ± 0.0050	0.78	0.826	0.1293 ± 0.0027	1.36	0.147	0.0461 ± 0.0018
0.39	0.529	0.2274 ± 0.0037	0.78	0.803	0.1289 ± 0.0038	1.56	0.469	0.0431 ± 0.0016
0.39	0.308	0.1947 ± 0.0038	0.78	0.710	0.1259 ± 0.0025	1.56	0.257	0.0380 ± 0.0016
0.51	0.897	0.2256 ± 0.0046	0.78	0.510	0.1114 ± 0.0027	1.56	0.145	0.0384 ± 0.0013
0.58	0.895	0.1899 ± 0.0038	0.78	0.290	0.1054 ± 0.0023	1.75	0.454	0.0328 ± 0.0010
0.58	0.855	0.1923 ± 0.0038	0.78	0.167	0.0984 ± 0.0021	1.75	0.248	0.0328 ± 0.0013
0.58	0.837	0.1866 ± 0.0036	0.97	0.796	0.0949 ± 0.0019	1.75	0.138	0.0303 ± 0.0018
0.58	0.833	0.1836 ± 0.0037	0.97	0.745	0.0968 ± 0.0021	1.95	0.243	0.0246 ± 0.0013

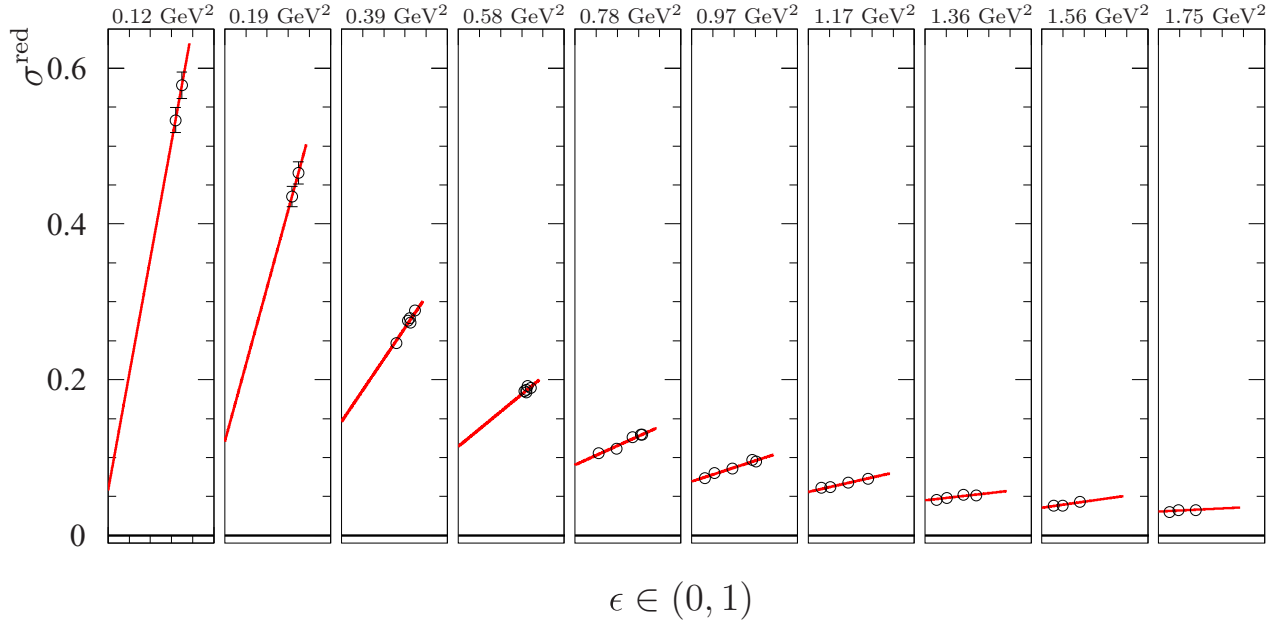


FIG. 9. Same as Fig. 6, but for data from Ref. [54].

TABLE VIII. Reduced cross sections from Ref. [11].

Q^2 (GeV ²)	ϵ	σ_{red}	Q^2 (GeV ²)	ϵ	σ_{red}
0.65	0.682	0.15452 ± 0.00099	3.75	0.403	0.00599 ± 0.00012
0.65	0.919	0.17305 ± 0.00108	3.75	0.658	0.00620 ± 0.00012
0.65	0.955	0.17646 ± 0.00115	3.75	0.826	0.00616 ± 0.00014
0.90	0.549	0.09835 ± 0.00010	4.25	0.257	0.00421 ± 0.00015
0.90	0.810	0.10843 ± 0.00010	4.25	0.553	0.00448 ± 0.00021
0.90	0.931	0.11098 ± 0.00008	4.25	0.786	0.00456 ± 0.00013
2.20	0.488	0.02048 ± 0.00011	5.25	0.469	0.00250 ± 0.00002
2.20	0.783	0.02158 ± 0.00010	5.25	0.702	0.00255 ± 0.00001
2.20	0.924	0.02168 ± 0.00013	5.25	0.659	0.00259 ± 0.00002
2.75	0.284	0.01243 ± 0.00012			
2.75	0.673	0.01295 ± 0.00011			
2.75	0.896	0.01329 ± 0.00012			

TABLE IX. Reduced cross section from Ref. [56].

Q^2 (GeV ²)	ϵ	σ_{red}	Q^2 (GeV ²)	ϵ	σ_{red}
1.00	0.692	0.08833 ± 0.00182	2.50	0.620	0.01580 ± 0.00033
1.00	0.869	0.09301 ± 0.00196	2.50	0.723	0.01617 ± 0.00034
1.00	0.930	0.09579 ± 0.00200	2.50	0.800	0.01619 ± 0.00032
2.00	0.634	0.02527 ± 0.00053	2.50	0.846	0.01633 ± 0.00035
2.00	0.735	0.02606 ± 0.00053	2.50	0.949	0.01683 ± 0.00034
2.00	0.808	0.02652 ± 0.00053	2.50	0.963	0.01714 ± 0.00045
2.00	0.877	0.02662 ± 0.00057	3.01	0.623	0.01026 ± 0.00022
2.00	0.938	0.02649 ± 0.00081	3.01	0.761	0.01053 ± 0.00022
2.00	0.953	0.02745 ± 0.00059	3.01	0.910	0.01070 ± 0.00034
2.00	0.963	0.02767 ± 0.00059	3.01	0.932	0.01090 ± 0.00024
2.00	0.968	0.02753 ± 0.00093	3.01	0.951	0.01106 ± 0.00034

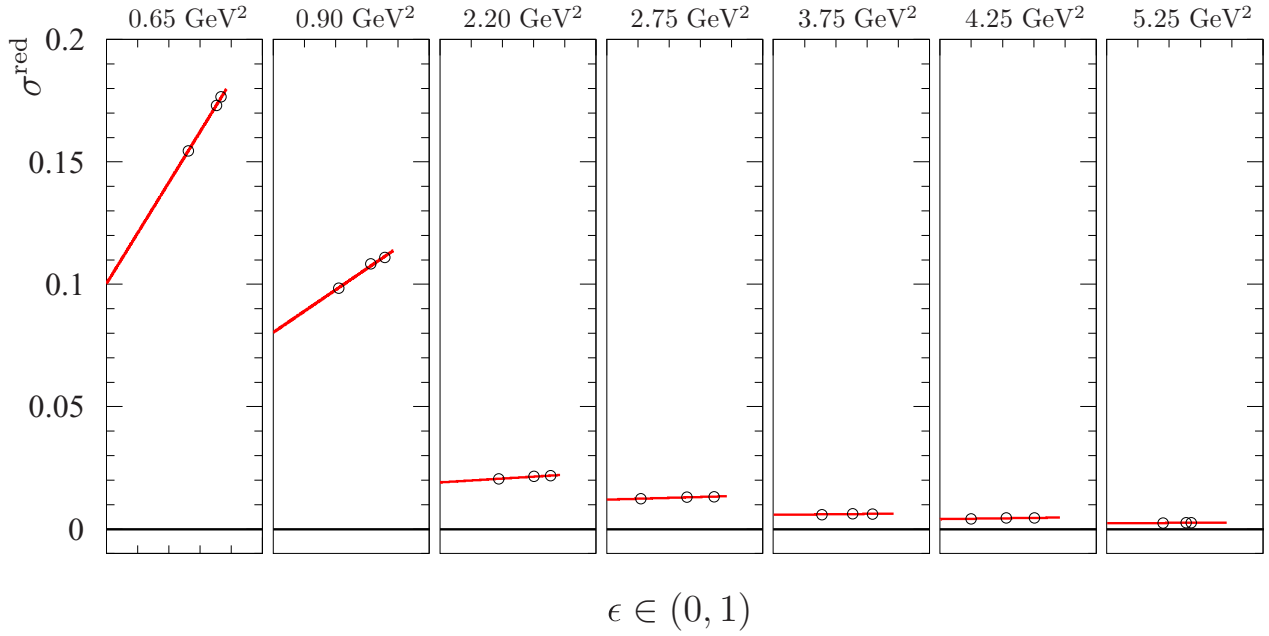


FIG. 10. Same as Fig. 6 but for data from Ref. [11].

APPENDIX G: FIT OF THE DATA OF REF. [56]

Table IX reports the original data from Ref. [56]. Fits to these data for the four Q^2 values are shown in Fig. 11.

APPENDIX H: FIT OF THE DATA OF REF. [9]

Table X reports the original data from Ref. [9]. Fits to these data for the five Q^2 values are shown in Fig. 12.

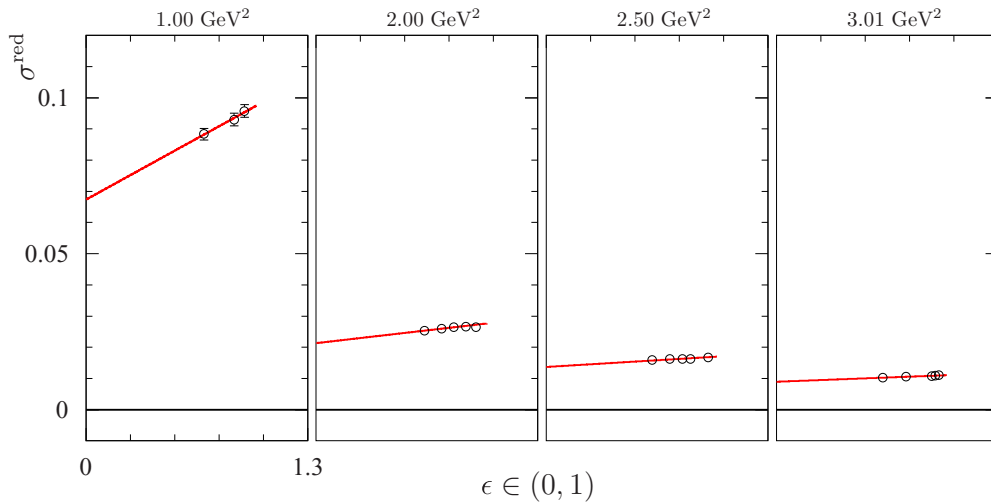


FIG. 11. Same as Fig. 6, but for data from Ref. [56].

TABLE X. Reduced cross sections from Ref. [9].

Q^2 (GeV ²)	ϵ	σ_{red}	Q^2 (GeV ²)	ϵ	σ_{red}
1.00	0.955	0.09527 ± 0.00133	2.50	0.903	0.01618 ± 0.00027
1.00	0.932	0.09398 ± 0.00141	2.50	0.803	0.01596 ± 0.00028
1.00	0.918	0.09701 ± 0.00150	2.50	0.732	0.01602 ± 0.00029
1.50	0.969	0.04928 ± 0.00073	2.50	0.960	0.01665 ± 0.00023
1.50	0.880	0.04788 ± 0.00083	2.50	0.932	0.01692 ± 0.00034
1.50	0.853	0.04743 ± 0.00074	2.50	0.824	0.01639 ± 0.00029
2.00	0.952	0.02779 ± 0.00047	2.50	0.733	0.01573 ± 0.00029
2.00	0.877	0.02651 ± 0.00043	2.50	0.672	0.01578 ± 0.00029
2.00	0.814	0.02611 ± 0.00063	3.75	0.953	0.00639 ± 0.00009
2.00	0.772	0.02641 ± 0.00045	3.75	0.922	0.00641 ± 0.00001
2.50	0.960	0.01641 ± 0.00023	3.75	0.646	0.00601 ± 0.00012

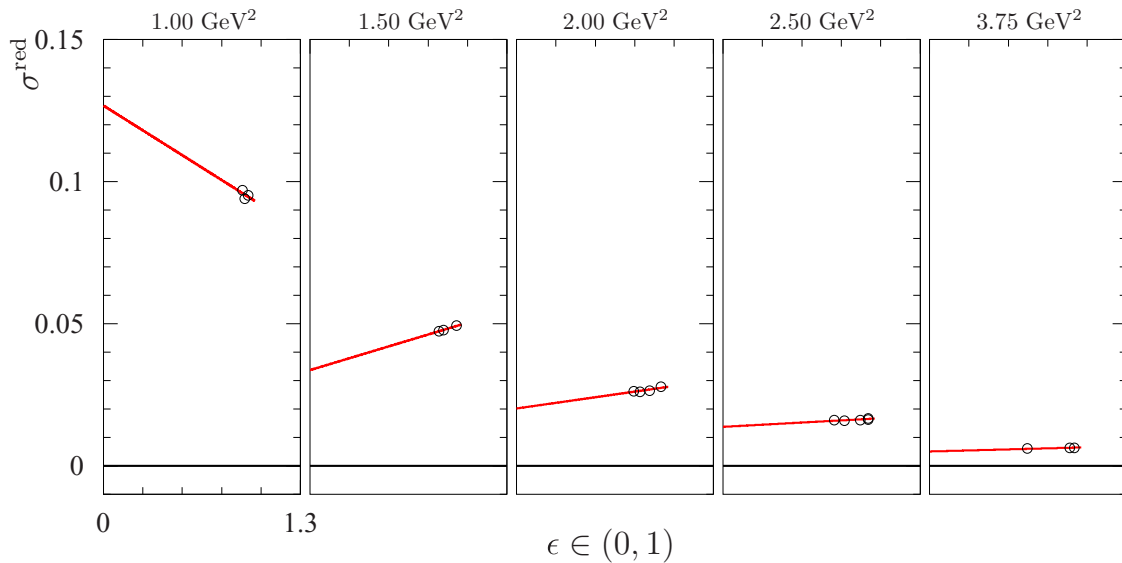


FIG. 12. Same as Fig. 6, but for data from Ref. [9].

TABLE XI. Reduced cross sections from Ref. [10].

Q^2 (GeV ²)	ϵ	σ_{red}	Q^2 (GeV ²)	ϵ	σ_{red}
2.64	0.117	0.01322 ± 0.00007	3.20	0.443	0.00893 ± 0.00005
2.64	0.355	0.01375 ± 0.00008	3.20	0.696	0.00916 ± 0.00005
2.64	0.597	0.01407 ± 0.00008	3.20	0.813	0.00937 ± 0.00005
2.64	0.781	0.01443 ± 0.00008	4.10	0.160	0.00466 ± 0.00003
2.64	0.865	0.01462 ± 0.00008	4.10	0.528	0.00490 ± 0.00003
3.20	0.131	0.00858 ± 0.00005	4.10	0.709	0.00501 ± 0.00003

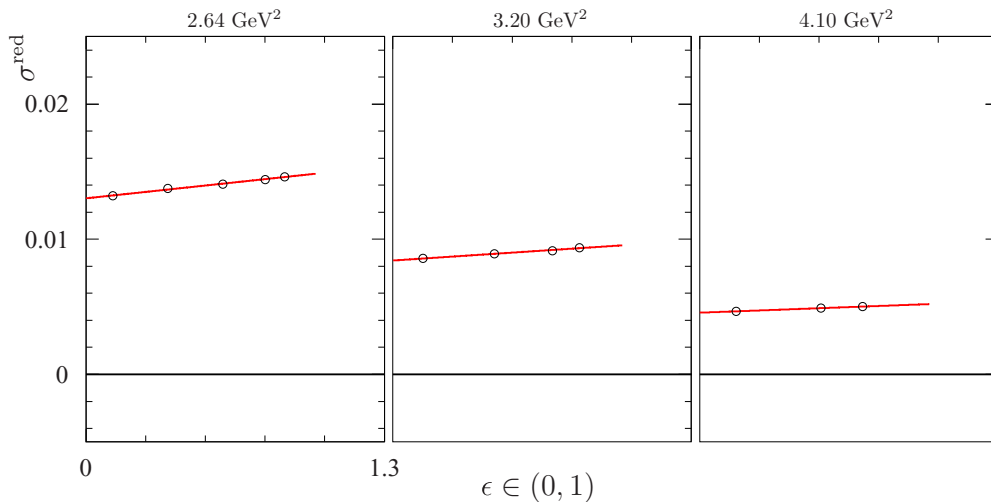


FIG. 13. Same as Fig. 6, but for data from Ref. [10].

APPENDIX I: FIT OF THE DATA OF REF. [10]

Table XI reports the original data from Ref. [10]. Fits to these data for the three Q^2 values are shown in Fig. 13.

-
- [1] V. Matveev, R. Muradian, and A. Tavkhelidze, *Lett. Nuovo Cim.* **7**, 719 (1973).
- [2] S. J. Brodsky and G. R. Farrar, *Phys. Rev. Lett.* **31**, 1153 (1973).
- [3] M. Rosenbluth, *Phys. Rev.* **79**, 615 (1950).
- [4] W. Bartel *et al.*, *Nucl. Phys. B* **58**, 429 (1973).
- [5] L. E. Price, J. R. Dunning, M. Goitein, K. Hanson, T. Kirk, and R. Wilson, *Phys. Rev. D* **4**, 45 (1971).
- [6] K. M. Hanson, J. R. Dunning, M. Goitein, T. Kirk, L. E. Price, and R. Wilson, *Phys. Rev. D* **8**, 753 (1973).
- [7] F. Borkowski, G. Simon, V. Walther, and R. Wendling, *Nucl. Phys. B* **93**, 461 (1975).
- [8] D. H. Coward *et al.*, *Phys. Rev. Lett.* **20**, 292 (1968).
- [9] J. Litt *et al.*, *Phys. Lett. B* **31**, 40 (1970).
- [10] I. Qattan *et al.*, *Phys. Rev. Lett.* **94**, 142301 (2005).
- [11] M. Christy *et al.* (E94110 Collaboration), *Phys. Rev. C* **70**, 015206 (2004).
- [12] F. Iachello, A. Jackson, and A. Lande, *Phys. Lett. B* **43**, 191 (1973).
- [13] G. Holzwarth, *Z. Phys. A* **356**, 339 (1996).
- [14] N. Kroll, T. Lee, and B. Zumino, *Phys. Rev.* **157**, 1376 (1967).
- [15] A. Akhiezer and M. Rekalov, *Sov. Phys. Dokl.* **13**, 572 (1968).
- [16] A. Akhiezer and M. Rekalov, *Sov. J. Part. Nucl.* **4**, 277 (1974).
- [17] A. Puckett *et al.*, *Phys. Rev. C* **85**, 045203 (2012).
- [18] E. J. Brash, A. Kozlov, S. Li, and G. M. Huber, *Phys. Rev. C* **65**, 051001 (2002).
- [19] L. W. Mo and Y.-S. Tsai, *Rev. Mod. Phys.* **41**, 205 (1969).
- [20] L. C. Maximon and J. A. Tjon, *Phys. Rev. C* **62**, 054320 (2000).
- [21] A. V. Gramolin and D. M. Nikolenko, *Phys. Rev. C* **93**, 055201 (2016).
- [22] R. E. Gerasimov and V. S. Fadin, *Yad. Fiz.* **78**, 73 (2015) [*Phys. Atom. Nucl.* **78**, 69 (2015)].
- [23] E. A. Kuraev and V. S. Fadin, *Yad. Fiz.* **41**, 733 (1985) [*Sov. J. Nucl. Phys.* **41**, 466 (1985)].
- [24] Y. M. Bystritskiy, E. A. Kuraev, and E. Tomasi-Gustafsson, *Phys. Rev. C* **75**, 015207 (2007).
- [25] E. A. Kuraev, Yu. M. Bystritskiy, A. I. Ahmadov, and E. Tomasi-Gustafsson, *Phys. Rev. C* **89**, 065207 (2014).
- [26] V. N. Boitsov, L. A. Kondratyuk, and V. B. Kopeliovich, *Yad. Fiz.* **16**, 515 (1972) [*Sov. J. Nucl. Phys.* **16**, 287 (1973)].
- [27] F. M. Lev, *Yad. Fiz.* **23**, 1350 (1976) [*Sov. J. Nucl. Phys.* **21**, 145 (1975)].
- [28] V. Franco, *Phys. Rev. D* **8**, 826 (1973).
- [29] M. P. Rekalov, E. Tomasi-Gustafsson, and D. Prout, *Phys. Rev. C* **60**, 042202 (1999).
- [30] P. A. M. Guichon and M. Vanderhaeghen, *Phys. Rev. Lett.* **91**, 142303 (2003).
- [31] M. P. Rekalov and E. Tomasi-Gustafsson, *Eur. Phys. J. A* **22**, 331 (2004).
- [32] M. Rekalov and E. Tomasi-Gustafsson, *Nucl. Phys. A* **740**, 271 (2004).
- [33] M. Rekalov and E. Tomasi-Gustafsson, *Nucl. Phys. A* **742**, 322 (2004).
- [34] G. Gakh and E. Tomasi-Gustafsson, *Nucl. Phys. A* **761**, 120 (2005).
- [35] G. Gakh and E. Tomasi-Gustafsson, *Nucl. Phys. A* **771**, 169 (2006).
- [36] D. Y. Chen, H. Q. Zhou, and Y. B. Dong, *Phys. Rev. C* **78**, 045208 (2008).
- [37] H.-Q. Zhou and B.-S. Zou, *Nucl. Phys. A* **883**, 49 (2012).
- [38] G. Gakh and E. Tomasi-Gustafsson, *Nucl. Phys. A* **838**, 50 (2010).
- [39] J. Arrington, W. Melnitchouk, and J. A. Tjon, *Phys. Rev. C* **76**, 035205 (2007).
- [40] E. Tomasi-Gustafsson, M. Osipenko, E. Kuraev, and Y. Bystritskiy, *Phys. Atom. Nucl.* **76**, 937 (2013).
- [41] W. Alberico, S. Bilenky, C. Giunti, and K. Graczyk, *J. Phys. G* **36**, 115009 (2009).

- [42] E. Tomasi-Gustafsson and G. I. Gakh, *Phys. Rev. C* **72**, 015209 (2005).
- [43] A. V. Afanasev, S. J. Brodsky, C. E. Carlson, Y.-C. Chen, and M. Vanderhaeghen, *Phys. Rev. D* **72**, 013008 (2005).
- [44] D. Borisyuk and A. Kobushkin, *Phys. Rev. C* **78**, 025208 (2008).
- [45] N. Kivel and M. Vanderhaeghen, *Phys. Rev. Lett.* **103**, 092004 (2009).
- [46] A. V. Gramolin *et al.*, *Nucl. Phys. Proc. Suppl.* **225–227**, 216 (2012).
- [47] R. G. Milner (OLYMPUS Collaboration), *AIP Conf. Proc.* **1441**, 159 (2012).
- [48] R. P. Bennett, *AIP Conf. Proc.* **1441**, 156 (2012).
- [49] E. Tomasi-Gustafsson, *Phys. Part. Nucl. Lett.* **4**, 281 (2007).
- [50] J. Arrington, *Phys. Rev. C* **68**, 034325 (2003).
- [51] L. Andivahis *et al.*, *Phys. Rev. D* **50**, 5491 (1994).
- [52] S. Pacetti, R. Baldini Ferroli, and E. Tomasi-Gustafsson, *Phys. Rep.* **550**, 1 (2015).
- [53] T. Janssens, R. Hofstadter, E. B. Hughes, and M. R. Yearian, *Phys. Rev.* **142**, 922 (1966).
- [54] C. Berger, V. Burkert, G. Knop, B. Langenbeck, and K. Rith, *Phys. Lett. B* **35**, 87 (1971).
- [55] R. Bijker and F. Iachello, *Phys. Rev. C* **69**, 068201 (2004).
- [56] R. C. Walker *et al.*, *Phys. Rev. D* **49**, 5671 (1994).
- [57] R. E. Taylor, in Proceedings of the International Symposium on Electron and Photon Interactions at High Energies, SLAC, Stanford University, 1967, pp. 78–101 <http://www-public.slac.stanford.edu/sciDoc/docMeta.aspx?slacPubNumber=SLAC-PUB-0372>.
- [58] P. N. Kirk *et al.*, *Phys. Rev. D* **8**, 63 (1973).